https://doi.org/10.31925/farmacia.2026.4.13 **ORIGINAL ARTICLE**

THERAPEUTIC MECHANISM OF ACTION OF SEA BUCKTHORN EXTRACT IN MOUSE MODEL OF PSORIASIS COMORBID WITH NONALCOHOLIC FATTY LIVER DISEASE

WENHAO YIN, KANG GE, YIHUI XIE, MENGZHU JIN *

Department of Dermatology, The First Hospital of Jiaxing/Affiliated Hospital of Jiaxing University, Jiaxing, 314001, China

**corresponding author: jmz_1001@126.com*

Manuscript received: May 2026

Abstract

This study investigated the therapeutic mechanism of sea buckthorn extract (SBE) in a mouse model of psoriasis (PSO) associated with nonalcoholic fatty liver disease (NAFLD). Seventy male C57BL/6 mice were assigned to PSO, NAFLD, and PSO+NAFLD groups. Following model establishment, mice received either normal saline (NS) or SBE, generating six experimental subgroups. Liver function, lipid metabolism parameters, histopathological changes, inflammatory mediators, and PI3K/AKT/FOXO1 signaling pathway proteins were evaluated. Compared with the PSO group, PSO+NAFLD mice exhibited increased skin fold thickness, higher Baker scores, elevated cutaneous TNF-α, IL-17, IL-6, and IL-23 expression, and enhanced phosphorylation of PI3K, AKT, and FOXO1 ($p < 0.05$). Relative to the NAFLD group, PSO+NAFLD mice showed aggravated liver injury, increased NAFLD activity scores, elevated AST, ALT, TC, TG, and LDL-C levels, reduced HDL-C, increased hepatic inflammatory cytokines, and activation of the PI3K/AKT/FOXO1 pathway ($p < 0.05$). SBE administration significantly ameliorated these alterations. These findings indicate that PSO and NAFLD mutually exacerbate inflammation and metabolic dysfunction, while SBE alleviates disease severity by suppressing inflammatory responses and modulating the PI3K/AKT/FOXO1 signaling pathway.

Rezumat

Studiul a investigat efectul terapeutic al extractului de cătină (Sea Buckthorn Extract - SBE) într-un model murin de psoriazis (PSO) asociat cu boala ficatului gras nonalcoolic (NAFLD). Șaptezeci de șoareci masculi C57BL/6 au fost repartizați în grupurile PSO, NAFLD și PSO+NAFLD. După inducerea modelelor experimentale, animalele au primit fie soluție salină normală (NS), fie SBE, rezultând șase subgrupuri experimentale. Au fost evaluate: funcția hepatică, parametrii metabolismului lipidic, modificările histopatologice, mediatorii inflamatori și proteinele implicate în calea de semnalizare PI3K/AKT/FOXO1. Comparativ cu grupul PSO, șoarecii din grupul PSO+NAFLD au prezentat o creștere a grosimii pliului cutanat, scoruri Baker mai mari, niveluri crescute ale TNF-α, IL-17, IL-6 și IL-23 la nivelul pielii, precum și o fosforilare accentuată a proteinelor PI3K, AKT și FOXO1 ($p < 0,05$). În raport cu grupul NAFLD, șoarecii PSO+NAFLD au prezentat leziuni hepatice mai severe, scoruri crescute ale activității NAFLD, valori mai mari ale AST, ALT, colesterolului total, trigliceridelor și LDL-colesterolului, niveluri reduse de HDL-colesterol, expresie crescută a citokinelor inflamatorii hepatice și activarea căii PI3K/AKT/FOXO1 ($p < 0,05$). Administrarea SBE a ameliorat semnificativ aceste modificări. Rezultatele indică faptul că asocierea PSO și NAFLD agravează inflamația și tulburările metabolice, iar SBE reduce severitatea afecțiunilor prin inhibarea răspunsului inflamator și modularea căii de semnalizare PI3K/AKT/FOXO1.

Keywords: psoriasis, nonalcoholic fatty liver disease, sea buckthorn extract, inflammation, PI3K/AKT/FOXO1 pathway

Introduction

Psoriasis (PSO) is a chronic inflammatory skin disease characterized by epidermal thickening with erythema and scale. There is a proven association between PSO and obesity/metabolic disorders, including metabolic syndrome, dyslipidemia, and diabetes (1). Chronic inflammation related to metabolic disorders is believed to exacerbate PSO by activating inflammatory responses (2). Nonalcoholic fatty liver disease (NAFLD) increases the risk of cardiovascular disease, diabetes, and chronic kidney disease (3, 4). In recent years, PSO has been considered an extrahepatic complication of NAFLD, with a significantly increased prevalence in the NAFLD population (5). Moreover, the severity of PSO in patients with NAFLD is often higher than in non-NAFLD patients (6). Additionally, the incidence of NAFLD in PSO patients is twice that of the healthy population (7). Therefore, a bidirectional relationship between PSO and NAFLD is believed to exist, although the underlying causal relationship has not yet been elucidated. Sea buckthorn is a plant that is both medicinal and edible, with effects of strengthening the spleen, aiding digestion, relieving cough, expectorating phlegm, and activating blood circulation to remove blood stasis. It contains flavonoids, sugars, vitamins, oils, and fatty acids, with antioxidant, anticancer, anti-inflammatory, lipid-lowering, and blood sugar-lowering

effects (8-10). Balkrishna *et al*. (11) found that oral and topical application of sea buckthorn oil in PSO-like mouse models significantly reduced ear thickness and skin lesion scores. Boca *et al*. (12) applied sea buckthorn extract (SBE) topically to skin lesions in 10 PSO patients, with improvements in psoriasis area and severity index (PASI) and dermatology life quality index scores at 4 and 8 weeks. During NAFLD, TNF-α and IL-6 promote the progression of steatosis to steatohepatitis, while TGF-β activates hepatic stellate cells, leading to liver fibrosis (13). Liu *et al*. (14) found that SBE can exert anti-inflammatory properties. Additionally, Li *et al*. (15) found that ω-7 sea buckthorn oil can regulate lipid metabolism in hyperlipidemic mice, reducing hepatic steatosis, cholesterol accumulation, oxidative stress, and inflammatory responses, and can be used as a dietary supplement or therapeutic intervention for NAFLD management. Nishida and Morita (16) identified 180 potential targets for sea buckthorn triterpenic acids in treating NAFLD through network pharmacology, and found that it can lower serum lipid levels in NAFLD mice and improve epididymal fat and hepatic fat accumulation. In summary, sea buckthorn has effects on regulating lipid metabolism, anti-inflammatory actions, and improving PSO skin lesions. However, whether SBE can be used for the treatment of PSO comorbid with NAFLD still requires more evidence.

In this study, the mouse model of PSO comorbid with NAFLD was prepared, and the pathological changes in the skin and liver of comorbid mice were analyzed. SBE was administered by gavage, and the potential mechanisms affecting its therapeutic effects were further explored based on the PI3K/AKT/FOXO1 pathway. This study aims to provide reference materials for understanding the pathogenic links between PSO and NAFLD and investigating the potential therapeutic mechanisms of SBE in treating PSO comorbid with NAFLD.

Materials and Methods

Animals

Seventy male C57BL/6 mice (6 - 8 weeks old; approximately 20 g; Shanghai SLAC, China) were housed in a strictly controlled SPF barrier environment: 20 - 26°C, relative humidity 40 - 70%, and 12-h photoperiod. The mice were given unrestricted access to sterilized complete nutrition feed and acidified drinking water. They were kept in an independent ventilation caging system with bedding, nesting materials, and shelters. All procedures complied with animal welfare guidelines and were reviewed and approved by the Institutional Animal Care and Use Committee of Affiliated Hospital of Jiaxing University.

Establishment of animal model

PSO model: A PSO-like skin mouse model was established using Imiquimod (IMQ) cream. The specific method involved depilating the dorsal skin of the mice and applying 62.5 mg of 5% IMQ cream (Sichuan Mingxin Pharmaceutical Co., Ltd., China) evenly to the skin surface once daily for 7 consecutive days. The modelling effect was evaluated based on the morphological changes of skin lesions and histopathological alterations. Morphological changes included the appearance of punctate erythema and scale on days 2–3 after IMQ induction, skin folding on day 4, and the formation of PSO-like plaques with a film phenomenon and punctate bleeding on days 6–8, which basically resolved by day 14. Histopathological changes included early hyperkeratosis with parakeratosis, reduction of the granular layer, and acanthosis and on days 7 - 8, the pathological features were significant, including Munro microabscesses, club-shaped epidermal projections, dermal inflammatory cell infiltration, and capillary dilation, which then gradually recovered.

NAFLD model: The NAFLD mouse model was established. The specific method involved feeding the mice with high-fat diet (8 consecutive weeks). The formula included 80% regular feed (flour 25%, cornmeal 30%, bran 15%, fishmeal 8%, bone meal 3%, milk powder 2%, soybean meal 11%, salt 0.5%, cod liver oil 0.5%, eggs 4%, vitamins, and inorganic salts 1%), 16% lard, 2% cholesterol, and 2% porcine bile salts (sourced from Jiaxing Traditional Chinese Medicine Hospital (Jiaxing, China)). The modeling effect was evaluated based on the morphological and histopathological changes of the liver. Morphological changes included enlarged volume, yellowish color, blunt edges, and greasy texture. Histopathological changes included hepatocyte swelling with diffuse large and small lipid droplet vacuoles in the cytoplasm, causing nuclear displacement or disappearance, and significant inflammatory infiltration.

PSO and NAFLD comorbidity model: The mice were first fed with high-fat diet (8 consecutive weeks), and from the 7th week, IMQ cream was applied to the dorsal skin once daily for 7 days. The modelling effect was then evaluated based on the morphological and histopathological changes of skin lesions and liver.

Grouping and treatments

Seventy male C57BL/6 mice were randomly divided into 7 groups, with 10 mice in each group. The different groups and their respective interventions were as follows: (1) Normal control (NC) group: They were fed a standard diet and housed under conventional conditions, receiving normal saline at 10 mL/kg bw *via* oral gavage once daily; (2) Psoriasis model + normal saline (PSO+NS) group: The psoriasis model was established using IMQ cream. After successful modelling, the mice were administered

normal saline at 10 mL/kg bw *via* oral gavage once daily; (3) Psoriasis model + sea buckthorn extract (PSO+SBE) group: The psoriasis model was established using IMQ cream. After successful modelling, the mice were administered SBE at 10 mL/kg bw *via* oral gavage once daily; (4) Non-alcoholic fatty liver disease model + normal saline (NAFLD+NS) group: The NAFLD model was established by feeding a high-fat diet. After successful modelling, the mice were administered normal saline at 10 mL/kg bw *via* oral gavage once daily; (5) Non-alcoholic fatty liver disease model + sea buckthorn extract (NAFLD+SBE) group: The NAFLD model was established by feeding a high-fat diet. After successful modelling, the mice were administered Sea Buckthorn Extract (SBE) at 10 mL/kg bw *via* oral gavage once daily; (6) Comorbidity model + normal saline (PSO+NAFLD +NS) group: The comorbidity model was established by first inducing the NAFLD model with a high-fat diet, followed by inducing the psoriasis model with imiquimod (IMQ) cream. After successful modeling, the mice were administered normal saline at 10 mL/kg bw *via* oral gavage once daily; (7) Comorbidity model + sea buckthorn extract (PSO+NAFLD +SBE) group: The comorbidity model was established by first inducing the NAFLD model with a high-fat diet, followed by inducing the psoriasis model with IMQ cream. After successful modeling, the mice were administered normal saline at 10 mL/kg bw via oral gavage once daily.

In the above experimental process, SBE was sourced from Jiaxing Traditional Chinese Medicine Hospital (Jiaxing, China), mainly containing sea buckthorn fruit oil and total flavonoids. It was dissolved in fresh distilled water to prepare a suspension containing 400 mg/kg SBE, which was stored in a refrigerator at 4°C for later use. The intervention scheme is illustrated in Figure 1.

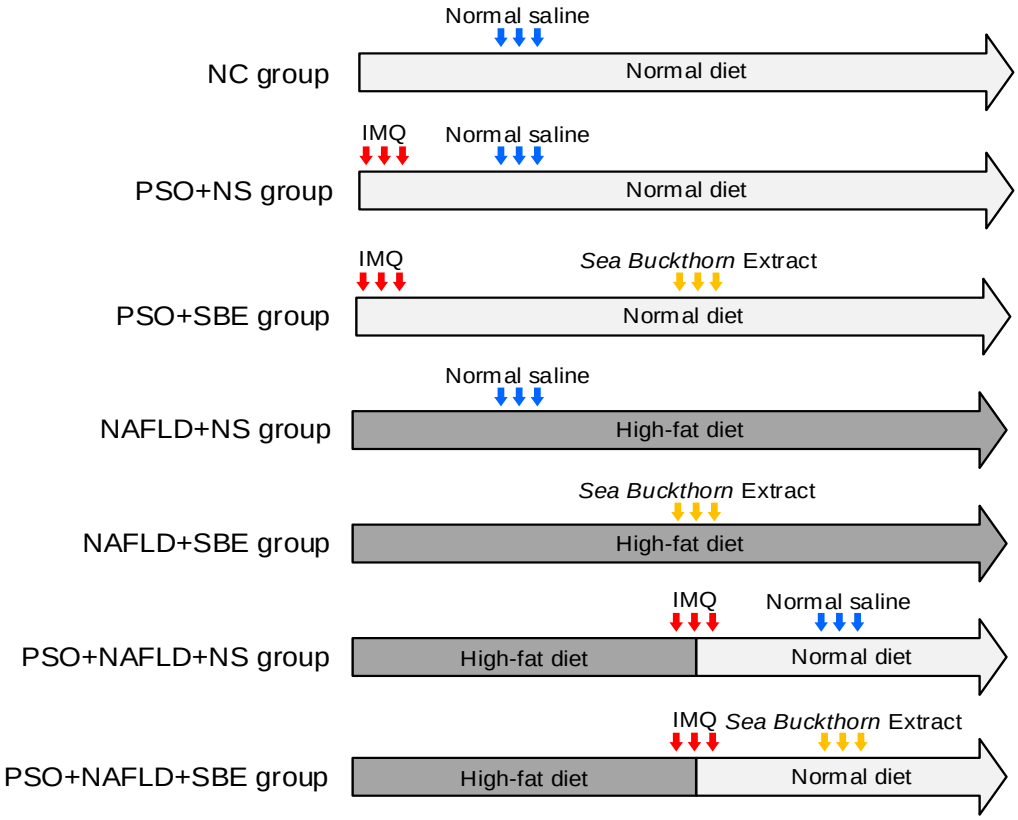

Figure 1.
Intervention scheme

Sample collection and processing

After the final gavage treatment, the mice were fasted overnight and mildly anesthetized with 1.5% isoflurane (Hubei Norna Technology Co., Ltd., China) under an oxygen flow rate of 0.8 - 1.0 L/min using an anesthesia machine. Blood was collected from the retro-orbital sinus, and after centrifugation (3000 rpm, 10 min), the serum was used for biochemical analysis. The liver and dorsal skin lesions were harvested after euthanasia (cervical dislocation). The tissues were weighed, with a portion stored at -80°C for later use and another portion fixed in 10% formalin (Shanghai Beyotime Biotechnology Co., Ltd., China) for histopathological examination.

Psoriasis area and severity index (PASI) scoring

To quantify the severity of PSO-like lesions, a modified PASI scoring system (17) was used for assessment at the following time points: day 0, day 1, day

3, day 5, day 7, and day 14. The scoring system evaluated the dorsal skin lesions based on two dimensions: severity and the percentage of affected area. The severity included erythema, scale, and skin thickening, with each parameter scored on a scale of 0 - 4 (none to severe). The percentage of affected area was estimated and scored accordingly. The final score was a composite of the individual parameter scores and area coefficients, with higher scores indicating more severe disease.

Hematoxylin and Eosin (H&E) staining

Subsequent to fixation in 10% formalin, dorsal skin and liver tissues were processed: (1) paraffin embedding, (2) sectioning at 3 - 5 μm, and (3) H&E staining (Shanghai Beyotime Biotechnology Co., Ltd., China). A single blinded researcher observed the histopathological changes and scored them under a Ci-E optical microscope (Nikon, Japan). The histopathological evaluation of dorsal skin lesions used the Baker score (18), with criteria as follows: (1) Munro micro abscess in the stratum corneum scored 2, parakeratosis scored 1, and hyperkeratosis scored 0.5; (2) thinning or disappearance of the granular layer scored 1; (3) acanthosis scored 1; (4) elongated and mildly undulating epidermal projections scored 0.5, moderately undulating scored 1, and severely undulating scored 1.5; (5) mild mononuclear and polymorphonuclear cell infiltration in the dermis scored 0.5, moderate scored 1, severe scored 2, dermal papilla protrusion scored 0.5, and capillary dilation scored 0.5. The histopathological evaluation of liver tissue used the NAFLD activity score (NAS) (19), with criteria as follows: (1) fat deposition < 5% scored 0, 5 - 33% scored 1, 34 - 66% scored 2, > 66% scored 3; (2) no lobular inflammation scored 0, < 2 inflammatory foci in a 200× field of view scored 1, 2 - 4 foci scored 2, > 4 foci scored 3; (3) no hepatocyte ballooning degeneration scored 0, minimal ballooning degeneration scored 1, and marked or extensive ballooning degeneration scored 2.

Biochemical analysis of blood samples

Total cholesterol (TC), aspartate aminotransferase (AST), low- and high-density lipoprotein cholesterol (LDL-C and HDL-C), triglycerides (TG), and alanine aminotransferase (ALT) were determined using an XL-300 fully automated biochemical analyzer (Erba, Germany).

RT-qPCR

RNA extraction from dorsal skin and liver tissues was carried out. After measuring RNA concentration and purity with a UV-visible spectrophotometer, cDNA was synthesized according to the reverse transcription kit instructions. A 20 μL reaction system was set up for quantitative PCR amplification of target genes using cDNA as the template. Primer sequences were as follows:

IL-6: 5'-GGCGGATCGGATGTTGTGAT-3', 5'-3';
IL-17: 5'-TGAAAACACAGAAGTAACGTCCG-3', 5'-CCCAGGAGGAAATTGTAATGGGA-3';
IL-23: 5'-AATAATGTGCCCCGTATCCAGT-3', 5'-GCTCCCCTTTGAAGATGTCAG-3';
TNF-α: 5'-GTCCTGCTCTACGTGACGAG-3', 5'-TCTCTCCTTTTCTGCCATCTCT-3';
GAPDH: 5'-AATGGATTTGGACGCATTGGT-3', 5'-TTTGCACTGGTACGTGTTGAT-3'.

The amplification program was set as: 95℃ 2 min→95℃ 15 s→60℃ 20 s→72℃ 20 s→72℃ 5 min → 4℃ Hold, 40 cycles. Data were analyzed using Light Cycler Software version 3.5 (Roche, Switzerland), with GAPDH as the internal reference and relative expression levels of target genes calculated using the $2^{-\triangle\triangle Ct}$ method. All reagent kits were purchased from Applied Biosystems (USA).

Western blotting

Protein concentration was determined according to the BCA kit (Merck Life Science, USA) instructions. Subsequently, 5 μL of protein was loaded for separation by polyacrylamide gel electrophoresis at 100 V for 1.5 h. The separated proteins were transferred to a nitrocellulose membrane (Merck Life Science, USA) and blocked at 25℃ for 2 h. Rabbit anti-PI3K, -p-PI3K, -AKT, -p-AKT, -FOXO1, -p-FOXO1, and mouse anti-β-actin (Abcam, UK) primary antibodies were added (4℃, approximately 16 h). Secondary antibodies conjugated with horseradish peroxidase (Abcam, UK) were applied (25℃, 1 h). Enhanced chemiluminescence reagent (Thermo Fisher Scientific, USA) was added, followed by development with a ChemiDoc MP device (Bio-Rad, USA). Image J software was adopted (National Institutes of Health, USA), with β-actin as the internal reference for calculating the relative gray values of target proteins.

Statistical analysis

All data were reported in the format of mean ± SD. Independent samples *t*-tests and one-way ANOVA were adopted. GraphPad Prism 9 software (GraphPad Software, USA) was applied. Differences with $p < 0.05$ were regarded as statistically significant.

Results and Discussion

Morphological changes of skin

The PASI scores were significantly increased in the PSO+NS and PSO+NAFLD+NS groups compared to NC group ($p < 0.05$), while significantly decreased in the PSO+SBE group compared to the PSO+NS group ($p < 0.05$) and in the PSO+NAFLD+SBE group compared to PSO+NAFLD+NS group ($p < 0.05$) (Figure 2).

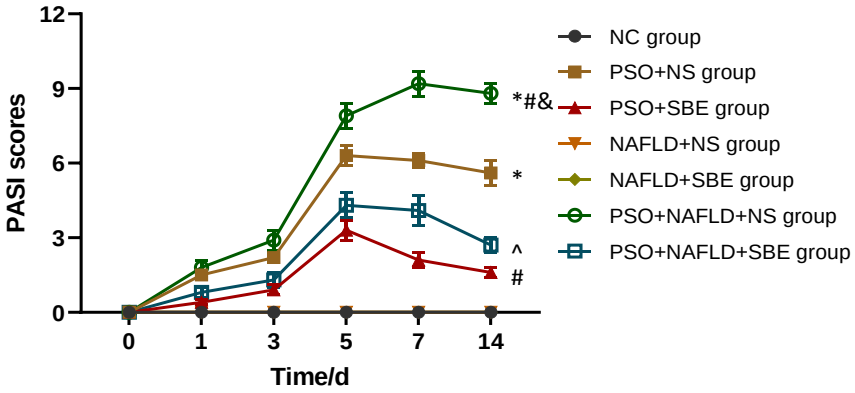

Figure 2.
Comparison of PASI scores on the dorsal skin of mice across different groups. * $p < 0.05$ *vs.* NC group; # $p < 0.05$ *vs.* PSO+NS group; & $p < 0.05$ *vs.* NAFLD+NS group; ^ $p < 0.05$ *vs.* PSO+NAFLD+NS group

There was no significant difference in skin fold thickness among the NC, NAFLD+NS, and NAFLD+SBE groups ($p > 0.05$). Skin fold thickness was noticeably increased in the PSO+NS and PSO+NAFLD+NS groups compared to NC group ($p < 0.05$), while it was noticeably reduced in the PSO+SBE group compared to the PSO+NS group ($p < 0.05$) and in the PSO+NAFLD+SBE group compared to the PSO+NAFLD+NS group ($p < 0.05$) (Figures 3A and 3B). The Baker scores were significantly increased in the PSO+NS and PSO+NAFLD+NS groups compared to NC group ($p < 0.05$), while it was significantly decreased in the PSO+SBE group compared to the PSO+NS group ($p < 0.05$) and in the PSO+NAFLD +SBE group compared to the PSO+NAFLD+NS group ($p < 0.05$) (Figure 3C).

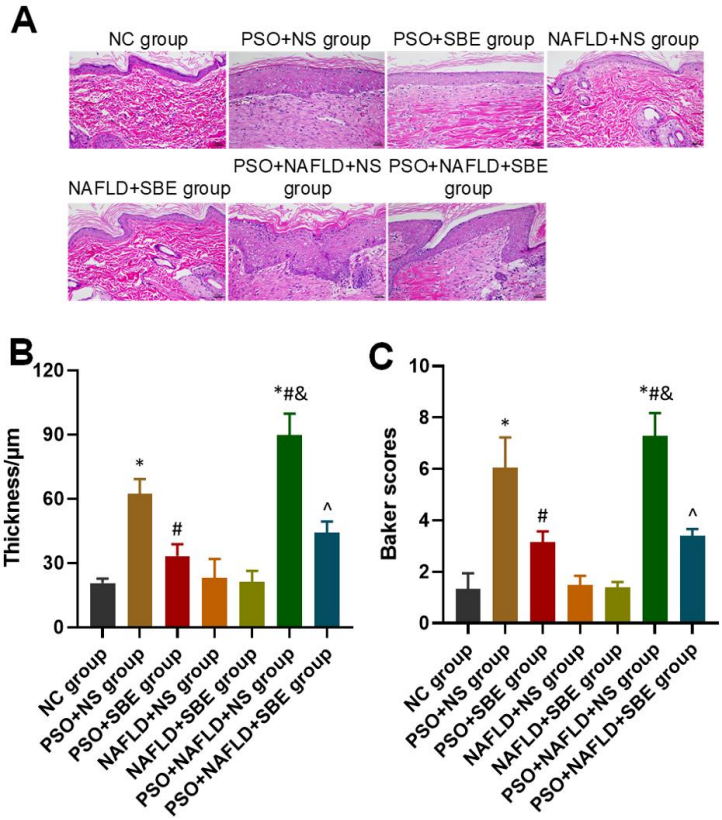

Figure 3.
Contrast of skin pathological morphology. A: Observation of skin H&E staining, 200×; B: Skin fold thickness; C: Skin Baker scores. * $p < 0.05$ *vs.* NC group; # $p < 0.05$ *vs.* PSO+NS group; & $p < 0.05$ *vs.* NAFLD+NS group; ^ $p < 0.05$ *vs.* PSO+NAFLD+NS group

Liver morphology

Ballooning degeneration of hepatocytes, along with lipid droplet deposition and inflammatory cell infiltration, was observed in the liver tissues of mice from the NAFLD+NS and PSO+NAFLD+NS groups (Figure 4A). In contrast, the severity of lipid droplet deposition and inflammatory cell infiltration was markedly improved in the liver tissues of mice from the NAFLD+SBE and PSO+NAFLD+SBE groups (Figure 4A). The NAFLD activity score (NAS) was significantly increased in the NAFLD+NS and PSO+NAFLD+NS groups compared to the NC group ($p < 0.05$), while the NAS was significantly decreased in the NAFLD+SBE group compared to the NAFLD+NS group and in the PSO+NAFLD +SBE group compared to the PSO+NAFLD+NS group ($p < 0.05$) (Figure 4B).

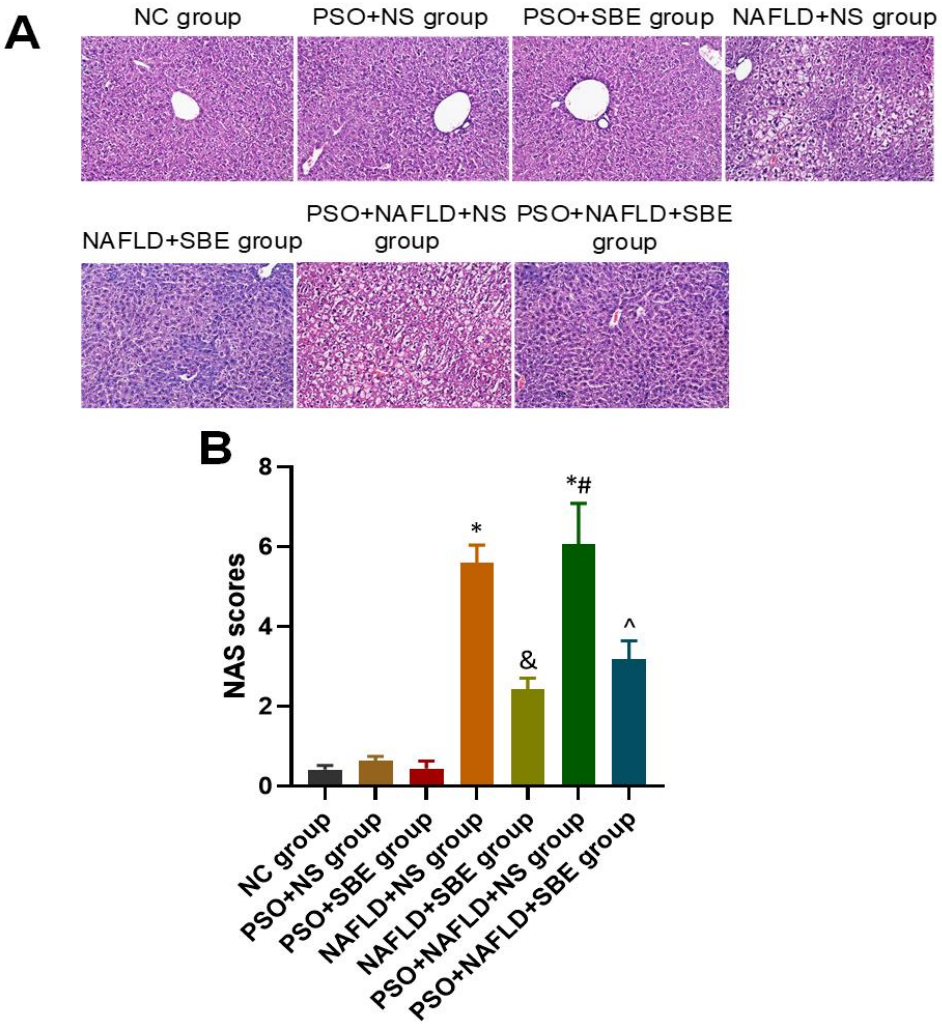

Figure 4.

Contrast of liver pathological morphology. A: Observation of liver H&E staining, 200×; B: Liver NAS scores. *$p < 0.05$ *vs*. NC group; $^{\#}$ $p < 0.05$ *vs*. PSO+NS group; $^{\&}$ $p < 0.05$ *vs*. NAFLD+NS group; ^ $p < 0.05$ *vs*. PSO+NAFLD+NS group

Serum biochemical indicators

No significant differences were observed in the serum levels of ALT, AST, TG, TC, LDL-C, and HDL-C among the NC, PSO+NS, and PSO+SBE groups ($p > 0.05$). Compared to the NC group, the NAFLD+NS and PSO+NAFLD+NS groups exhibited significantly increased serum levels of ALT, AST, TG, TC, and LDL-C, along with a significantly decreased level of HDL-C ($p < 0.05$). Compared to the NAFLD+NS group, the NAFLD+SBE group showed significantly decreased serum levels of ALT, AST, TG, TC, and LDL-C, and a significantly increased level of HDL-C ($p < 0.05$). Similarly, compared to the PSO+NAFLD+NS group, the PSO+NAFLD+SBE group demonstrated significantly reduced serum levels of ALT, AST, TG, TC, and LDL-C, and a significantly elevated level of HDL-C ($p < 0.05$) (Figure 5).

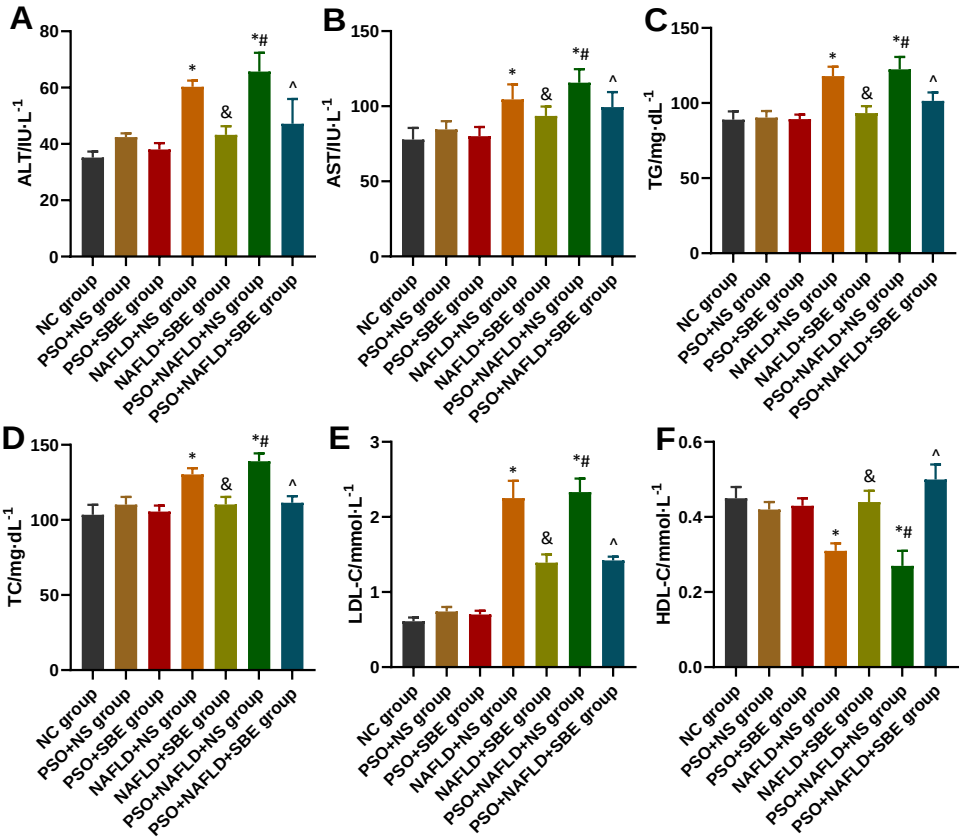

Figure 5.
Contrast of serum biochemical indicator levels. A: ALT; B: AST; C: TG; D: TC; E: LDL-C; F: HDL-C. *p < 0.05 *vs.* NC group; # p < 0.05 *vs.* PSO+NS group; & p < 0.05 *vs.* NAFLD+NS group; ^ p < 0.05 *vs.* PSO+NAFLD+NS group

Skin inflammatory cytokines

The expression levels of IL-6, IL-17, IL-23, and TNF-α in the skin were significantly increased in the PSO+NS and PSO+NAFLD+NS groups compared to the NC group (p < 0.05). Compared to both the PSO+NS and NAFLD+NS groups, the expression levels of IL-6, IL-17, IL-23, and TNF-α in the skin were significantly higher in the PSO+NAFLD+NS group (p < 0.05). Compared to the PSO+NS group, the expression levels of IL-6, IL-17, IL-23, and TNF-α were significantly decreased in the PSO+SBE group (p < 0.05). Compared to the PSO+NAFLD+NS group, the expression levels of IL-6, IL-17, IL-23, and TNF-α were significantly lower in the PSO+NAFLD+SBE group (p < 0.05) (Figure 6).

Liver inflammatory cytokines

The expression levels of IL-6, IL-17, IL-23, and TNF-α in the liver were significantly increased in the NAFLD+NS and PSO+NAFLD+NS groups compared to the NC group (p < 0.05). Compared to both the PSO+NS and NAFLD+NS groups, the hepatic expression levels of IL-6, IL-17, IL-23, and TNF-α were significantly higher in the PSO+NAFLD+NS group (p < 0.05). Compared to the NAFLD+NS group, the expression levels of IL-6, IL-17, IL-23, and TNF-α in the liver were significantly decreased in the NAFLD+SBE group (p < 0.05), while compared to the PSO+NAFLD+NS group, the hepatic expression levels of IL-6, IL-17, IL-23, and TNF-α were significantly lower in the PSO+NAFLD+SBE group (p < 0.05) (Figure 7)

PI3K/AKT/FOXO1 pathway-associated protein expression

The protein expression levels of p-PI3K, p-AKT, and p-FOXO1 in the skin were significantly increased in the PSO+NS and PSO+NAFLD+NS groups compared to the NC group (p < 0.05) and in the PSO+NAFLD+NS group compared to both the PSO+NS and NAFLD+NS groups (p < 0.05). The protein expression levels of p-PI3K, p-AKT, and p-FOXO1 in the skin were significantly decreased in the PSO+SBE group compared to the PSO+NS group (p < 0.05) and in the PSO+NAFLD+SBE group compared to the PSO+NAFLD+NS group (p < 0.05) (Figure 8).

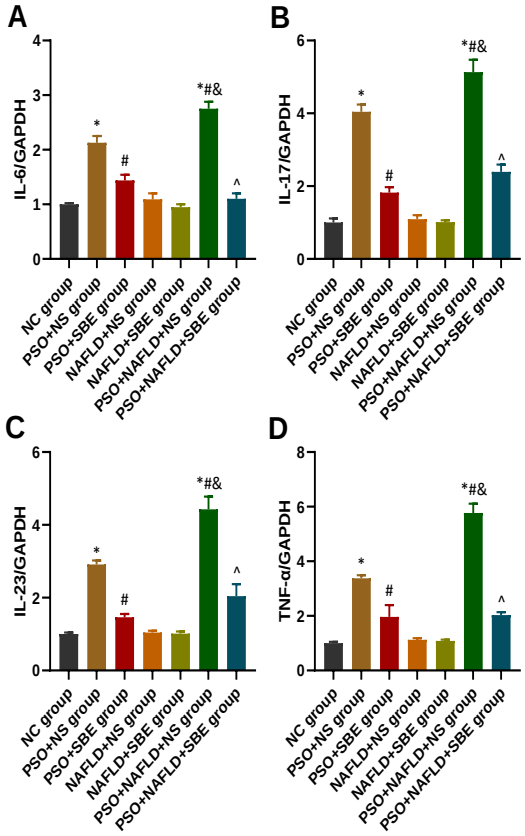

Figure 6.

Contrast of skin inflammatory gene expression. A: IL-6 relative expression; B: IL-17 relative expression; C: IL-23 relative expression; D: TNF-α relative expression. * $p < 0.05$ *vs*. NC group; $^{\#}$ $p < 0.05$ *vs*. PSO+NS group; $^{\&}$ $p < 0.05$ *vs*. NAFLD+NS group; ^ $p < 0.05$ *vs*. PSO+NAFLD+NS group

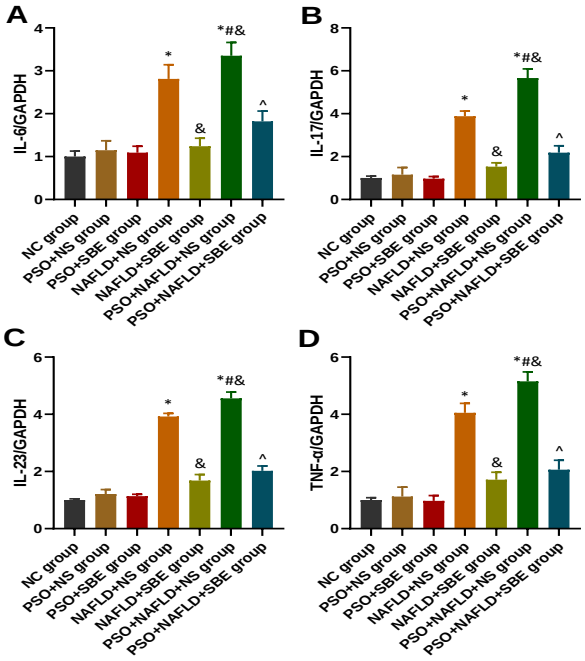

Figure 7.

Contrast of liver inflammatory gene expression. A: IL-6 relative expression; B: IL-17 relative expression; C: IL-23 relative expression; D: TNF-α relative expression. * $p < 0.05$ *vs*. NC group; $^{\#}$ $p < 0.05$ *vs*. PSO+NS group; & $p < 0.05$ *vs*. NAFLD+NS group; ^ $p < 0.05$ *vs*. PSO+NAFLD+NS group

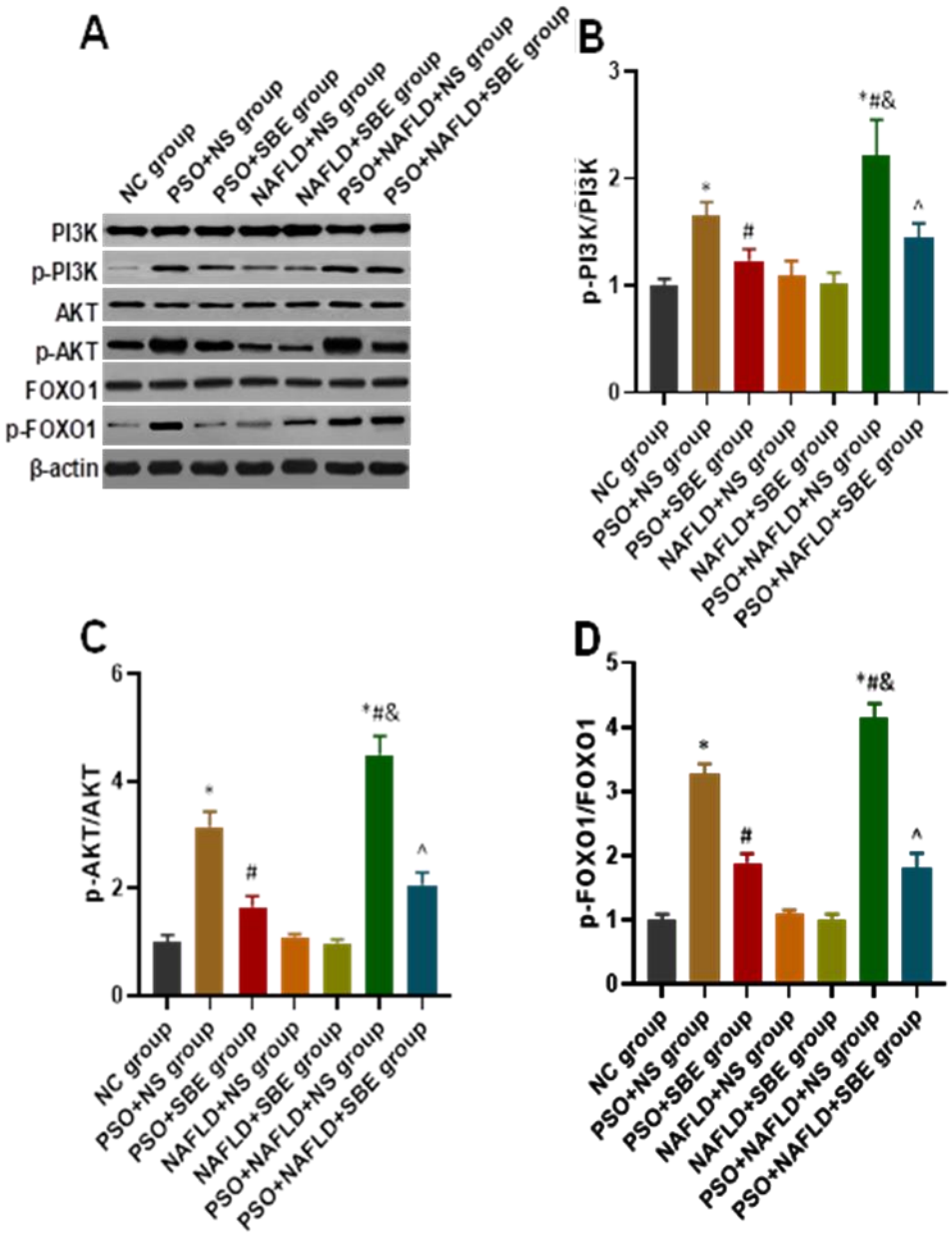

Figure 8.

Contrast of PI3K/AKT/FOXO1 pathway-associated protein expression in skin. A: western blotting; B: p-PI3K relative expression; C: p-AKT relative expression; D: p-FOXO1 relative expression. * $p < 0.05$ *vs*. NC group; # $p < 0.05$ *vs*. PSO+NS group; & $p < 0.05$ *vs*. NAFLD+NS group; ^ $p < 0.05$ *vs*. PSO+NAFLD+NS group

In Figure 9, compared to the NC group, In liver, the protein expression levels of p-PI3K, p-AKT, and p-FOXO1 were significantly increased in the NAFLD+NS and PSO+NAFLD+NS groups compared to the NC group ($p < 0.05$) and in the PSO+NAFLD+NS group compared to both the PSO+NS and NAFLD+NS groups ($p < 0.05$).The protein expression levels of p-PI3K, p-AKT, and p-FOXO1 in the liver were significantly decreased in the NAFLD+SBE group compared to the NAFLD+NS group and in the PSO+NAFLD+SBE group compared to the PSO+NAFLD+NS group ($p < 0.05$).

The study showed that the comorbidity of PSO and NAFLD increased the PASI score, skin fold thickness, and Baker score. Liver histopathological examination revealed ballooning degeneration and micro vesicular steatosis. In addition, the comorbidity of PSO and NAFLD exacerbated PSO skin symptoms, NAFLD progression, and inflammatory responses. It aligns with the conclusion of Takezaki *et al.* (20) that in mice comorbid with PSO and NAFLD, PSO skin symptoms were exacerbated, and levels of IL-23a in the skin and IL-17 and TNF-α in the serum were increased. In this study, although the levels of ALT, AST, TG, TC, and LDL-C were not significantly

elevated in mice comorbid with PSO and NAFLD, the NAS score was significantly increased. This may be due to the fact that in the preparation of the comorbid mouse model, IMQ induction occurred after the establishment of NAFLD and was of short duration. Therefore, the short duration of PSO induction was insufficient to effectively worsen the pathology of NAFLD. After gavage with SBE, the PASI score, skin fold thickness, Baker score, and NAS score were reduced in mice comorbid with PSO and NAFLD. The expression levels of inflammatory genes IL-6, IL-17, IL-23, and TNF-α in the skin and liver were significantly reduced.

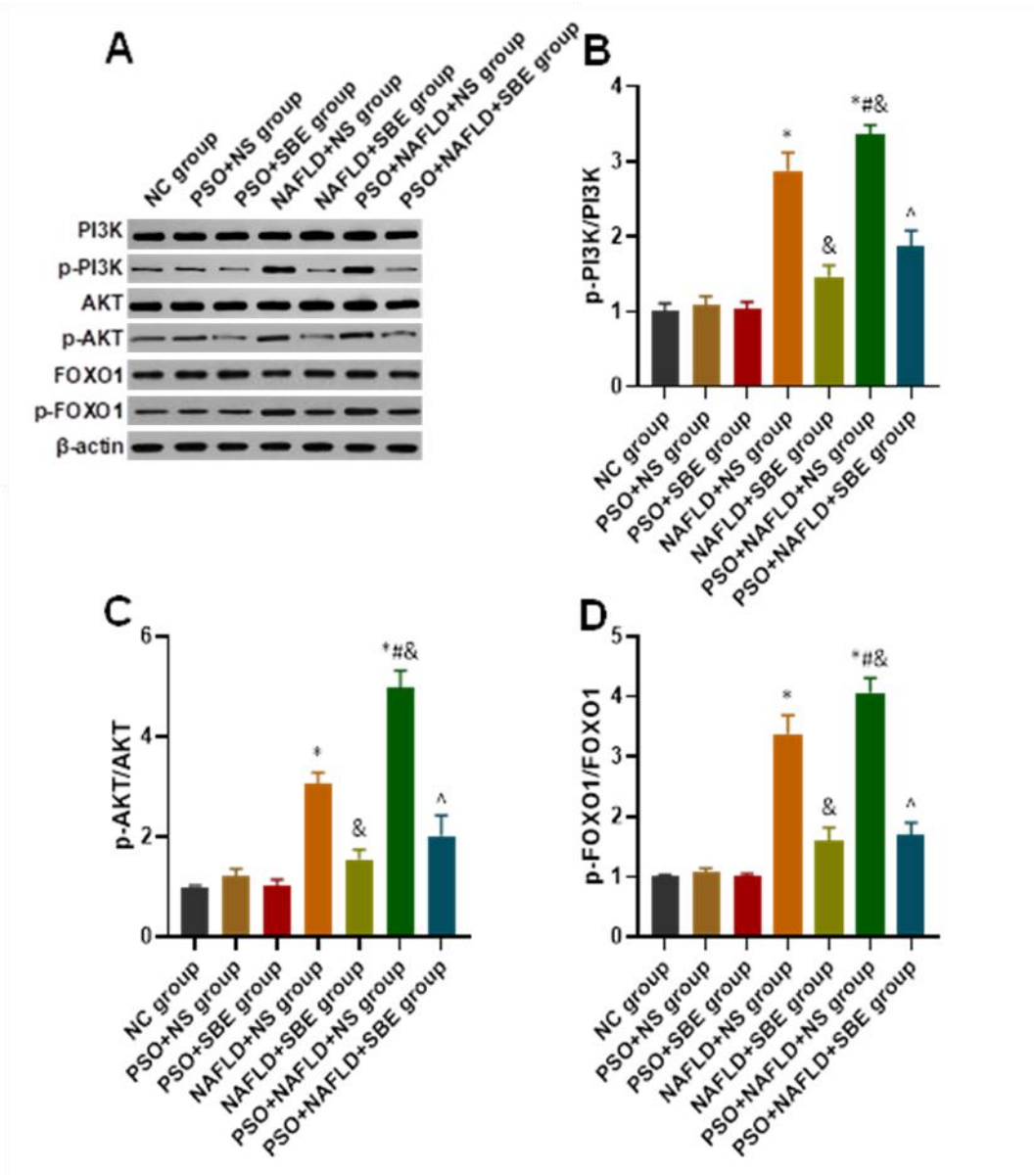

Figure 9.

Contrast of PI3K/AKT/FOXO1 pathway-associated protein expression in liver. A: western blotting; B: p-PI3K relative expression; C: p-AKT relative expression; D: p-FOXO1 relative expression. * $p < 0.05$ *vs*. NC group; # $p < 0.05$ *vs*. PSO+NS group; & $p < 0.05$ *vs*. NAFLD+NS group; ^ $p < 0.05$ *vs*. PSO+NAFLD+NS group

Elevated levels of pro-inflammatory cytokines in adipose tissue are one of the important characteristics of obesity and are closely related to insulin resistance and NAFLD (21). The increased TNF-α exacerbates the inflammatory response in metabolic syndrome (22). TNF-α in adipocytes and liver tissue can also act on the skin by promoting keratinocyte proliferation, inflammatory responses, and the secretion of vascular adhesion molecules, thereby worsening skin inflammation (23). The increased secretion of pro-inflammatory cytokines is a systemic factor associated with NAFLD and may also lead to the exacerbation of PSO-like skin phenotypes. Inflammation-promoting cytokines are involved in the

progression of PSO and NAFLD and are closely related to disease severity (24, 25). An elevated occurrence of NAFLD is observed in PSO population with more severe conditions (26). After gavage with SBE, the PSO skin and NAFLD liver pathological changes in the comorbid mouse model were significantly alleviated. Lipid metabolism improved, and inflammatory responses in the skin and liver were inhibited. It aligns with the conclusion of Sulthana *et al.* (27) that a sea buckthorn oil-based emulsion significantly improved erythema, desquamation, and inflammatory responses in an IMQ-induced PSO-like skin inflammation mouse model and also improved the PASI score. It is also similar to the findings of Sun *et al.* (28), who reported that SBE significantly reduced the liver index in the animal model and decreased lipid markers and liver function markers. This suggests that SBE can effectively improve PSO skin symptoms in mice comorbid with PSO and NAFLD and inhibit NAFLD progression by regulating lipid metabolism and reducing inflammatory responses.

The PI3K/AKT/FOXO1 pathway plays a pivotal role in regulating cell proliferation and apoptosis (29). In PSO lesions, inflammatory factors can activate PI3K, which further activates AKT. Phosphorylated AKT can induce the phosphorylation of downstream FOXO1, causing it to translocate from the nucleus to the cytoplasm and lose its transcriptional activity, thereby inducing abnormal proliferation of keratinocytes (30). Shen *et al.* (31) found that in a PSO cell model of keratinocyte HaCaT stimulated by a mixture of five pro-inflammatory cytokines, p-PI3K, p-AKT, and p-FOXO1 were noticeably upregulated. Ahmed *et al.* (32) found that in a diabetes-NAFLD rat model established by a high-fat diet and streptozotocin, the PI3K/AKT/FOXO1 pathway in the liver was also abnormally activated. This indicates that the activation of the PI3K/AKT/FOXO1 pathway is closely related to the occurrence of both PSO and NAFLD. This study found that after gavage with SBE, p-PI3K, p-AKT, and p-FOXO1 in the skin and liver tissues of mice comorbid with PSO and NAFLD were inhibited. It aligns with the conclusion of Wang *et al.* (33) that sea buckthorn oil can mediate the PI3K/AKT pathway to promote skin angiogenesis, thereby preventing and treating radiation-induced skin damage. Therefore, SBE has a therapeutic ability in the comorbidity of PSO and NAFLD by regulating the PI3K/AKT/FOXO1 pathway.

However, this study still has certain limitations. For example, the induction time of IMQ in the preparation of the comorbid mouse model is too short. A short induction time of IMQ can't assess its impact on liver fibrosis in mice. Vasseur *et al.* (34, 35) found that after 9 weeks of IMQ induction in a PSO model, liver fibrosis was accelerated. Yokogawa *et al.* (36) found that an induction time of more than 4 weeks with IMQ could lead to the occurrence of systemic lupus erythematosus-like dermatitis. Therefore, in the future, it is necessary to consider constructing transgenic PSO mouse models to further explore the relationship between PSO and NAFLD and analyze the potential mechanisms using techniques such as transcriptomics.

Conclusions

This study confirmed that the comorbidity of PSO and NAFLD exacerbates each other, leading to worsening skin lesions and lipid metabolism disorders. SBE can effectively improve the pathological changes in the skin and liver tissues, serum biochemical indicators, and inflammatory levels in comorbid mice, which is related to the inhibition of inflammatory mediators and the regulation of phosphorylation levels of the PI3K/AKT/FOXO1 pathway. Therefore, SBE shows certain intervention effects in improving the pathological changes related to the comorbidity of PSO and NAFLD, indicating its potential application value, but further experimental and clinical studies are needed for verification.

Acknowledgement

Not applicable.

Funding

This work was supported by Zhejiang Provincial Medical and Health Science and Technology Plan (2022KY1243) and Jiaxing Key Discipline of Medicine (2023-FC-006).

Availability of data and materials

The data generated in the present study are included in the figures and/or tables of this article.

Ethics approval and consent to participate

All experimental procedures were approved by Committee of Affiliated Hospital of Jiaxing University (No. JUMC 2021-168).

AI use disclosure

Not applicable.

Conflict of interest

The authors declare no conflict of interest.

References

1. Seiringer P, Hillig C, Schäbitz A, Jargosch M, Pilz AC, Eyerich S, et al. Spatial transcriptomics reveals altered lipid metabolism and inflammation-related gene expression of sebaceous glands in psoriasis and atopic dermatitis. Front Immunol. 2024;15:1334844.

2. Svedbom A, Mallbris L, González-Cantero Á, Playford M, Wu C, Mehta NN, et al. Skin inflammation, systemic inflammation, and cardiovascular disease in psoriasis. JAMA Dermatol. 2025;161(1):81-86.
3. Mladenova IL, Tan EF, Ng JY, Sharma P. Non-alcoholic fatty liver disease (NAFLD) and its association to cardiovascular disease: a comprehensive meta-analysis. JRSM Cardiovasc Dis. 2025;14:20480040251325929.
4. Dascalu AM, Serban D, Tanasescu D, Vancea G, Cristea BM, Stana D, et al. The value of white cell inflammatory biomarkers as potential predictors for diabetic retinopathy in type 2 diabetes mellitus (T2DM). Biomedicines. 2023;11(8):2106.
5. Xu S, Liu L, Li C, Ren Y, Zhang M, Xiang L, et al. Correlation among psoriasis, iridocyclitis, and non-alcoholic fatty liver disease: insights from Mendelian randomization and mediation analysis. Int J Med Sci. 2025;22(1):121-131.
6. Untaaveesup S, Kantagowit P, Ungprasert P, Kitlertbanchong N, Vajiraviroj T, Sutithavinkul T, et al. The risk of metabolic dysfunction-associated steatotic liver disease in moderate-to-severe psoriasis: a systematic review and meta-analysis. J Clin Med. 2025;14(4):1374.
7. González Fernández J, Prieto-Torres L, Martínez-Domínguez SJ, Barriendos Ambroj E, Ara Martín M. Triglyceride/glucose index combined with anthropometric parameters: a promising tool for screening NAFLD in patients with psoriasis. Actas Dermosifiliogr. 2025;116(7):T684-T691. [
8. Available in Spanish].
9. Chen Y, He W, Cao H, Wang Z, Liu J, Wang B, et al. Research progress of sea buckthorn (Hippophae rhamnoides L.) in prevention and treatment of cardiovascular disease. Front Cardiovasc Med. 2024;11:1477636.
10. Timnea O, Virgolici B, Gagniuc E, Mohora M, Miricescu D, Gradinaru D, et al. Outcome of co-administration of sea buckthorn fruit in high fat diet Wistar rats. Farmacia. 2024;72(3):581-587.
11. Zhu P, Ren Y, Wei C, Luo J, Wu D, Ye X, et al. Compounds from sea buckthorn and their application in food: a review. Food Chem. 2025;476:143428.
12. Balkrishna A, Sakat SS, Joshi K, Joshi K, Sharma V, Ranjan R, et al. Cytokines driven anti-inflammatory and anti-psoriasis like efficacies of nutraceutical sea buckthorn (Hippophae rhamnoides) oil. Front Pharmacol. 2019;10:1186.
13. Boca AN, Ilies RF, Saccomanno J, Pop R, Vesa S, Tataru AD, et al. Sea buckthorn extract in the treatment of psoriasis. Exp Ther Med. 2019;17(2):1020-1023.
14. Shu Y, Chu Y, Yang S, Cao J, Qiao Y, Zhao Y, et al. The integration of systematic pharmacology and experimental validation to explain the mechanism of action of Wuling capsule in the treatment of NAFLD. Comb Chem High Throughput Screen. 2025;28(9):1604-1623.
15. Liu C, Yi X, Li Y, Xu H, Wang P, Yang W, et al. Cianidanol from sea buckthorn exert anti-inflammatory effects by the inhibiting JAK2/STAT3 signaling pathway via an integrative pharmacology strategy. Plant Foods Hum Nutr. 2025;80(1):40.
16. Li J, Guo J, Yuen M, Yuen H, Peng Q. The comparative effects of ω-7 fatty acid-rich sea buckthorn oil and ω-3 fatty acid-rich DHA algal oil on improving high-fat diet-induced hyperlipidemia. Food Funct. 2025;16(4):1241-1253.
17. Nishida E, Morita A. The required absolute PASI score to achieve DLQI remission. J Dermatol. 2025;52(5):947-949.
18. Bhat L, Bhat SR, Ramakrishnan A, Amirthalingam M. Brilaroxazine lipogel displays antipsoriatic activity in imiquimod-induced mouse model. Skin Res Technol. 2024;30(2):e13606.
19. Lin J, Huang Y, Xu B, Gu X, Huang J, Sun J, et al. Effect of dapagliflozin on metabolic dysfunction-associated steatohepatitis: multicentre, double blind, randomised, placebo controlled trial. BMJ. 2025;389:e083735.
20. Ren L, Wang R, Wang Y, Tie F, Dong Q, Wang H, et al. Exploring the effect and mechanism of Hippophae rhamnoides L. triterpenoid acids on improving NAFLD based on network pharmacology and experimental validation in vivo and in vitro. J Ethnopharmacol. 2024;335:118657.
21. Takezaki D, Morizane S, Ikeda K, Iseki M, Sakamoto Y, Kawakami Y, et al. Co-occurrence of non-alcoholic steatohepatitis exacerbates psoriasis associated with decreased adiponectin expression in a murine model. Front Immunol. 2023;14:1214623.
22. Sharma A, Hakkak R, Gokden N, Joshi N, Parajuli N. Obesity-associated NAFLD coexists with a chronic inflammatory kidney condition that is partially mitigated by short-term oral metformin. Nutrients. 2025;17(13):2115.
23. Wen Y, Yi F, Zhang J, Wang Y, Zhao C, Zhao B, et al. Uncovering the protective mechanism of baicalin in treatment of fatty liver based on network pharmacology and cell model of NAFLD. Int Immunopharmacol. 2024;141:112954.
24. Shakya KR, Chatterjee N, Misra SK, Verma V. A bacterial cellulose-polydopamine based injectable hydrogel for enhanced hemostasis in acute wounds. Biomater Sci. 2025;13(12):3307-3324.
25. Cao J, Du T, He K, Dai Z, Xie X, Chen B, et al. Mendelian randomization and colocalization analysis reveal the role of IL-6 signaling pathway in psoriasis and potential therapeutic targets. Arch Dermatol Res. 2025;317(1):468.
26. Afrisham R, Alasvand G, Jadidi Y, Farrokhi V, Moradi N, Alizadeh S, et al. CCN3/NOV serum levels in non-alcoholic fatty liver disease (NAFLD) patients in comparison with the healthy group and its correlation with TNF-α and IL-6. Curr Mol Med. 2025;25(5):605-613.
27. van der Voort EA, Koehler EM, Nijsten T, Stricker BH, Hofman A, Janssen HL, et al. Increased prevalence of advanced liver fibrosis in patients with psoriasis: a cross-sectional analysis from the Rotterdam study. Acta Derm Venereol. 2016;96(2):213-217.
28. Sulthana S, Chary PS, Bhavana V, Pardhi E, Singh SB, Mehra NK. Development and evaluation emulgel for effective management of the imiquimod-induced psoriasis. Inflammopharmacology. 2023;31(1):301-320.
29. Sun S, Li B, Peng S, He L. Protective effect of sea buckthorn (Hippophae rhamnoides) extract on liver injury induced by high-fat diet in mice. Stud Health Technol Inform. 2023;308:605-610.
30. Abdou HM, Elmageed GMA, Hussein HK, Yamari I, Chtita S, El-Samad LM, et al. Antidiabetic effects of quercetin and silk sericin in attenuating dysregulation

of hepatic gluconeogenesis in diabetic rats through potential modulation of PI3K/Akt/FOXO1 signaling: in vivo and in silico studies. J Xenobiot. 2025;15(1):16.
31. Bui A, Liu J, Hong J, Hadeler E, Mosca M, Brownstone N, et al. Identifying novel psoriatic disease drug targets using a genetics-based priority index pipeline. J Psoriasis Psoriatic Arthritis. 2021;6(4):185-197.
32. Shen C, Liu X, Jia H, Wang W, Wang X, Wang H, et al. Application of bioinformatics analysis and molecular docking to study the mechanism of Qingying decoction in treating psoriasis. Hereditas. 2025;162(1):52.
33. Ahmed ES, Mohamed HE, Farrag MA. Luteolin loaded on zinc oxide nanoparticles ameliorates non-alcoholic fatty liver disease associated with insulin resistance in diabetic rats via regulation of PI3K/AKT/FoxO1 pathway. Int J Immunopathol Pharmacol. 2022;36:3946320221137435.
34. Wang Q, Cao B, Zhan J, Hu X, Yu Y, Li X, et al. Sea buckthorn oil promotes the PI3K-Akt-ERK signaling pathway and macrophage M2 polarization to reduce radiation-induced skin injury. Radiat Res. 2024;202(5):785-794.
35. Vasseur P, Pohin M, Jégou JF, Favot L, Venisse N, Mcheik J, et al. Liver fibrosis is associated with cutaneous inflammation in the imiquimod-induced murine model of psoriasiform dermatitis. Br J Dermatol. 2018;179(1):101-109.
36. Zugravu GS, Dimitriu DC, Ciobanu CP, Tamba BI, Ciorpac M, Mihai CT, et al. Benefits of sea buckthorn fruit oil as adjuvant therapy in rheumatoid arthritis. Farmacia. 2024;72(3):554-564.
37. Yokogawa M, Takaishi M, Nakajima K, Kamijima R, Fujimoto C, Kataoka S, et al. Epicutaneous application of toll-like receptor 7 agonists leads to systemic autoimmunity in wild-type mice: a new model of systemic lupus erythematosus. Arthritis Rheumatol. 2014;66(3):694-706.